

Chapter 10

Fatigue under Variable-Amplitude Loading

- 10.1 Introduction
 - 10.2 The Miner rule
 - 10.2.1 Effect of load cycles with stress amplitudes below the fatigue limit
 - 10.2.2 Effect of notch root plasticity
 - 10.2.3 Crack length at failure
 - 10.2.4 What is basically wrong with the Miner rule?
 - 10.3 Results of fatigue tests under VA loading
 - 10.4 Alternative fatigue life prediction methods for VA loading
 - 10.4.1 Damage calculations and extrapolation of S-N curves below the fatigue limit
 - 10.4.2 The relative Miner rule
 - 10.4.3 Strain history prediction model
 - 10.4.4 Predictions based on service-simulation fatigue tests
 - 10.5 Discussion of fatigue life predictions for VA loading
 - 10.5.1 Life estimates for a specific component and the Miner rule
 - 10.5.2 Considerations on the effect of the design stress level
 - 10.5.3 Comparison between different options for design improvements
 - 10.5.4 Comparison of different load spectra
 - 10.6 Major topics of the present chapter
- References

Symbols

- CA Constant-Amplitude
- VA Variable-Amplitude

*Predictions are difficult, especially on the future.
(Niels Bohr, Winston Churchill, Wim Kan)*

10.1 Introduction

Constant-amplitude (CA) fatigue loading is defined as fatigue under cyclic loading with a constant amplitude and a constant mean load. Sinusoidal loading is a classical example of CA fatigue loads applied in many fatigue tests. In the previous chapter on fatigue loads, it has been pointed out that various structures in service are subjected to variable-amplitude (VA) loading, which can be a rather complex load-time history, see several figures in Chapter 9. Predictions on fatigue life and crack growth should obviously be more complex than predictions for CA loading. The latter problem was discussed in Chapter 7 (Fatigue Lives of Notched Elements) and Chapter 8 (Crack Growth). In Chapter 7, the best defined problem was the prediction of the fatigue limit of a notched element. The fatigue limit is a threshold value of the stress amplitude. Stress amplitudes below this level do not lead to failure, while stress amplitudes above the fatigue limit lead to crack initiation and crack growth to failure. Rational arguments could be adopted for the predictions of the fatigue limit, by comparing fatigue limits of a structure to fatigue limits of simple unnotched specimens, but certain problems had to be recognized associated with the notch effect, size effect, surface effect and environmental influences.

For structures subjected to VA load cycles in service, it may be desirable that fatigue failures should never occur. It implies that all load cycles of the load spectra should not exceed the fatigue limit. The prediction problems is then restricted to the prediction of the fatigue limit as discussed in Chapter 7. However, this requirement can lead to a heavy structure and it can be unnecessarily conservative, especially if the number of more severe load cycles above the fatigue limit is relatively small. Moreover, a complete avoidance of fatigue is not always required. Failures after a sufficiently long life can be acceptable from an economical point of view, the more so if safety issues are not involved. Fatigue under VA load conditions is the subject of the present chapter. Possibilities for fatigue life predictions under VA loading are discussed, while predictions on crack growth under VA loading are covered in the following chapter (Chapter 11).

The discussion in Section 10.2 starts with considerations on the well-known Miner rule with its long lasting reputation. Reasons why and how this rule can be misleading are discussed. Results of various fatigue tests under VA loading are considered in Section 10.3. Alternative fatigue life prediction methods are reviewed in Section 10.4. A general discussion on the problems of fatigue life predictions for VA loading is presented in

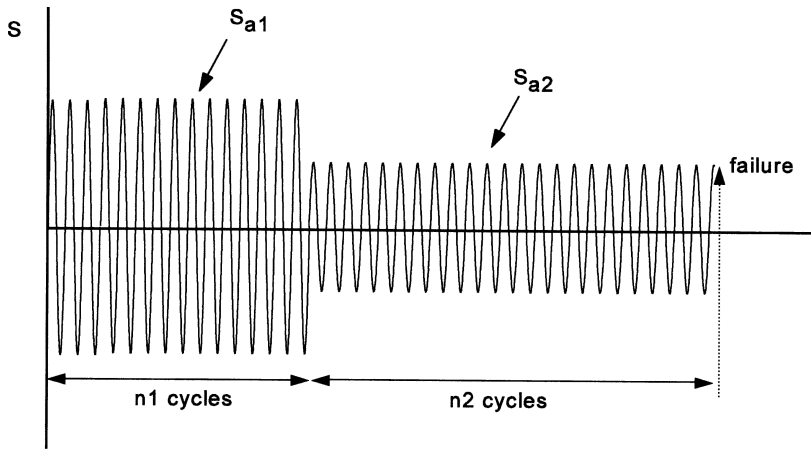


Fig. 10.1 A simple VA load sequence with two blocks of cycles.

Section 10.5. The major points of the present chapter are summarized in Section 10.6.

Several problems in this chapter are illustrated by test results of Al-alloys used in aircraft structures. The reason is that fatigue under VA loading has been extensively studied for these alloys in view of the significance of fatigue for the safety of aircraft. Load spectra measurements on aircraft in service have also widely been made for the same reason. It has stimulated the development of service-simulation fatigue tests. However, the experience of aircraft structures and materials is also relevant for other structures and materials, especially if these structures are made of relatively high-strength materials, which usually are fatigue sensitive.

10.2 The Miner rule

A specimen is fatigue tested under CA loading until a certain percentage of its fatigue life, say $x\%$. Fatigue damage must then be present in the specimen, because its original life (N) has been reduced to $(100 - x)\%$ of the fatigue life N . The damage may still be invisible, but it is present in the material of the specimen.

A most simple VA load history is presented in Figure 10.1. The amplitude is changed only once. Obviously, such a load history is not related to service load spectra, but it is considered here to discuss the basics of the Miner rule. Moreover, this simple VA load sequence was widely used in many older test

programs to check the validity of this rule. In Figure 10.1, n_1 cycles at a stress amplitude S_{a1} are applied, followed by cycles with an amplitude reduced to S_{a2} . The test is continued until failure occurs after n_2 cycles at the lower amplitude. Two different blocks of load cycles are thus applied in this test. The problem is to predict n_2 .

As early as 1924, Pålmgren [1] published the hypothesis which is now generally known as the Miner rule or the linear cumulative damage hypothesis. According to this rule, applying n_1 cycles with a stress amplitude S_{a1} and a corresponding fatigue life endurance N_1 , is equivalent to consuming n_1/N_1 of the fatigue resistance. The same assumption applies to any subsequent block of load cycles. Failure occurs if the fatigue resistance is fully consumed. For the two blocks in Figure 10.1, it implies that failure occurs at the moment that

$$\frac{n_1}{N_1} + \frac{n_2}{N_2} = 100\% \quad (10.1)$$

If more than two blocks are applied, this equation is generalized to read

$$\sum \frac{n_i}{N_i} = 1 \quad (10.2)$$

Pålmgren did not give any derivation, but he was in need of a rule in view of fatigue life calculations for ball-bearings under VA loading. He thus adopted the above simple assumption on fatigue damage accumulation. Langer in 1937 [2] postulated the same rule, but with a refinement, viz. the rule applies separately to the crack initiation period and to the crack growth period. Miner [3] in 1945 was the first one to propose a derivation of the linear cumulative damage rule. He assumed that the work that can be absorbed until failure has a constant value W , and in addition the work absorbed during n_i similar cycles is proportional to n_i . As a consequence, it implies that $w_i/W = n_i/N_i$. The criterion $\sum w_i = W$ then leads to Equation (10.2). Miner did VA experiments on unnotched specimens and a few riveted lap joints of 2024-T3 Alclad sheet material. He used two to four different blocks of load cycles in a test. He found $\sum n/N$ -values varying from 0.61 to 1.45, but on the average reasonably close to 1.0. Since that time, the rule $\sum n/N = 1$ has frequently been quoted as the Miner rule, the linear cumulative fatigue damage rule, or sometimes as the Pålmgren–Miner rule, although it would be more correct to refer to the Pålmgren rule. After 1945, numerous VA fatigue test programs were carried out to verify the Miner rule. In many cases, significant discrepancies were found which are discussed in Section 10.3. Stimulated by such discrepancies, several new theories on VA

fatigue were published. Unfortunately, similar to the validity of the Miner rule, the new theories did not have sufficient credibility from a physical point of view. Also, the experimental verification was quite often restricted to some specific test programs only. First, some essential comments will be made on a few principal inconsistencies of the Miner rule. Certain shortcomings of this rule must be understood in order to arrive at reasonable fatigue life considerations if VA load histories are applicable.

10.2.1 Effect of load cycles with stress amplitudes below the fatigue limit

If S_{a2} in the simple load sequence of Figure 10.1 is below the fatigue limit, then N_2 is infinite, and $n_2/N_2 = 0$. According to the Miner rule, the specimen will not fail because $\sum n/N = 1$ is never reached. In other words, according to the Miner rule, cycles with an amplitude below the fatigue limit are not damaging. This is physically inconsistent. Recall that cycles below the fatigue limit are unable to create a growing microcrack under CA loading, and thus can not cause failure, $N_2 = \infty$ and $n_2/N_2 = 0$. However, this argument is not relevant for VA loading. In the simple case of Figure 10.1, the cycles of the first block (n_1 cycles with amplitude S_{a1}) can create a growing crack. The question then is whether cycles of the second block can propagate this crack. In view of the stress singularity at the tip of the existing crack, a contribution to further crack growth is possible, which can indeed lead to failure. This also applies for more complex load histories including load cycle amplitudes above and below the fatigue limit. The Miner rule ignores the fatigue damage contribution of cycles below the fatigue limit to crack growth, because $N = \infty$. However, these cycles can contribute to an increase of existing fatigue damage.

The significance of the damage contribution of such small cycles depends on the type of load spectrum. Two highly different load spectra, previously shown in Figure 9.10, are presented again in Figure 10.2, together with an S-N curve. According to the Miner rule, all cycles with an amplitude below the fatigue limit should be non-damaging. Figure 10.2 illustrates that this number is very large for the steep spectrum and relatively small for the flat spectrum. In the first case (steep spectrum) the damage contribution of the small cycles should be expected to be significant, whereas in the second case (flat spectrum) it could be small.

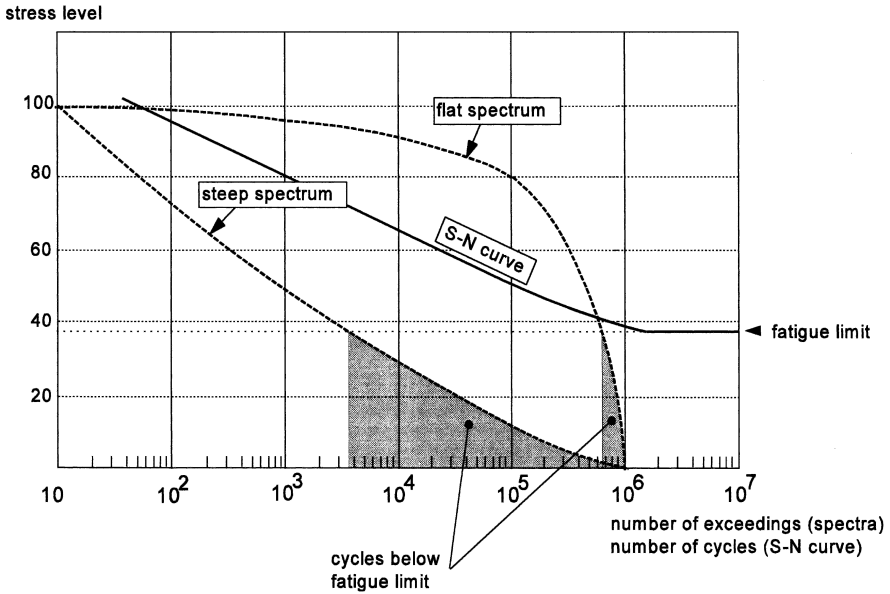


Fig. 10.2 The number of cycles below the fatigue limit depends on the shape of the load spectrum.

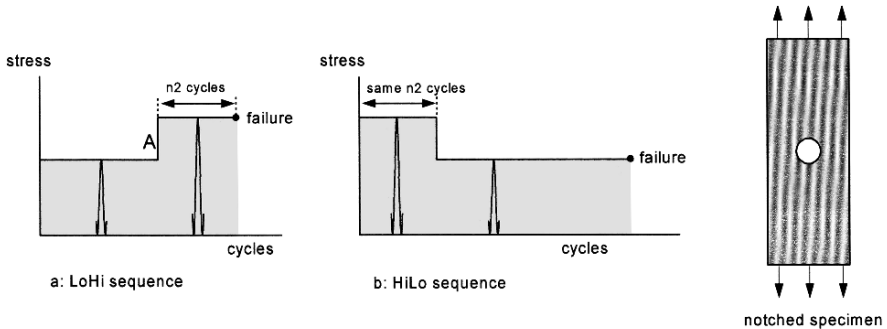


Fig. 10.3 Two different sequences of blocks in a simple VA load history ($R = 0$) applied to a notched specimen.

10.2.2 Effect of notch root plasticity

Two simple VA load sequences are shown in Figure 10.3. These sequences are applied to a notched specimen. The same two amplitudes are used in both sequences, but in the first sequence the test starts with the low amplitude (low-high sequence, or LoHi), and in the second one with the high amplitude (high-low sequence, or HiLo). The stress ratio is supposed

to be zero ($S_{min} = 0$, or $R = 0$). The following case is considered. The peak stress at the root notch (σ_{peak}) exceeds the yield stress ($S_{0.2}$) only in the block with the high amplitude, whereas this does not occur in the block with the low amplitude. It implies that notch root plasticity did not occur in the LoHi sequence (Figure 10.3a) during the low-amplitude cycles of the first block of the LoHi sequence. However, in the other sequence (HiLo, Figure 10.3b), notch root plasticity occurs immediately in the first block with the high amplitude. In this case, compressive residual stresses at the root of the notch are present at the beginning of the second block with the low-amplitude cycles. This is favorable for fatigue in the second block. Although the number of high-amplitude cycles (n_2) as observed in the LoHi test is applied in HiLo test, the fatigue life will be larger in this test due to the favorable residual stress. In other words, the sequence of the two blocks is significant for the fatigue life. This sequence effect is not predicted by the Miner rule because the rule ignores any change of residual stresses induced by previous cycles.

Another instructive example of experimental results is shown in Figure 10.4, again for a two-block VA fatigue test. In this case, the mean stress is zero in both blocks. The first block with a high amplitude is causing cyclic plasticity at the notch root because $K_t \cdot S_{a1} > S_{0.2}$. A subtle difference exists between the two HiLo sequences of Figures 10.4b and 10.4c. In the

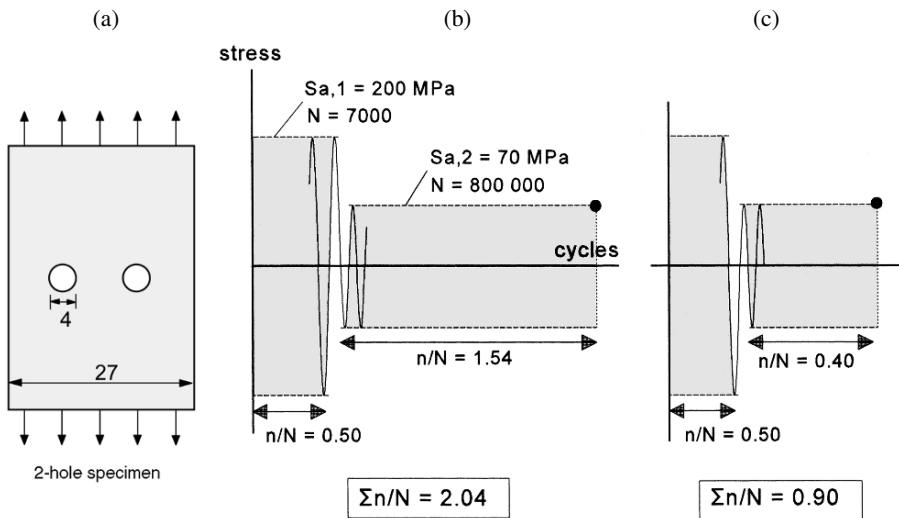


Fig. 10.4 Two-block VA tests on notched Al-alloy specimens [4]. Effect of compressive or tensile residual stress at the notch root in the second block.

first case the last maximum stress before reducing the amplitude is positive, and as a result it will leave a favorable negative residual stress at the notch. Consequently a longer life should be expected at S_{a2} . However, in the other case (Figure 10.4c), the opposite occurs. The last peak stress of the first block is negative, and it thus leaves an unfavorable residual tensile stress at the root notch, which shortens the fatigue life at S_{a2} . These trends are clearly reflected in the experimental results of $\sum n/N$ -values of 2.04 and 0.90 respectively. As said before, this plasticity induced sequence effect is not recognized by the Miner rule.

10.2.3 Crack length at failure

The two load sequences of Figure 10.3 are considered again. Assume that a crack length $a = 2$ mm (as an example) is reached at the end of the first low-amplitude block (point A in Figure 10.3), while the crack at this low amplitude could grow until $a = 20$ mm until failure occurs. However, a change to the second high-amplitude block could lead to immediate failure, because a small crack is more critical at a higher stress level. It obviously would lead to $\sum n/N < 1$. In the reversed sequence of Figure 10.3b, consider a transition made shortly before failure in the first block of the high amplitude, i.e. at the corresponding n/N slightly smaller than 1. In view of the high amplitude, the crack will be small just before failure. After the transition, substantial crack growth at the low amplitude of the second block is still possible before failure at the lower amplitude occurs at a relatively large crack length. A value $\sum n/N > 1$ should be expected.

10.2.4 What is basically wrong with the Miner rule?

Any cumulative damage rule requires a definition of fatigue damage. Following the discussion on the fatigue process in Chapter 2, it appears that a fatigue damage concept should include the crack length, or the amount of fatigue cracking. It could still be microcracking, nonetheless decohesion in the material. Keeping this aspect in mind, the third objection to the Miner rule, based on crack length at failure, is easily understood. According to the Miner rule, the fatigue damage at failure is $\sum n/N = 1$, or 100%. However, the crack length at failure depends on S_{\max} of the last load cycle. The Miner rule assumes that an S-N curve represents a curve of 100% fatigue damage.

That is not realistic because it is associated with a larger crack at a lower S_a -value, and a shorter crack at a higher S_a -value. An S-N curve is not a line of constant damage. Perhaps, this shortcoming of the Miner rule may not be so serious because the fatigue life spent in the macrocrack growth period is relatively short. However, the first objection (S_a below the fatigue limit being non-damaging) and the second one (residual stress effects at notches) can be very important. The fundamental shortcoming of the Miner rule is that fatigue damage is indicated by a single damage parameter only, viz. n/N , which accumulates from zero (pristine specimen) to 1 (failure).

As discussed in Chapter 2, fatigue cracking is an essential part of fatigue damage, starting with microcracking, followed by macrocracking. However, fatigue damage should be defined as embracing all changes in the material occurring as a result of the cyclic load. In addition to local decohesion (cracking), fatigue damage includes crack tip plasticity, local strain hardening in the crack tip zone, residual stresses around the crack tip, and for notched elements also macroplasticity at the root of the notch. It cannot be expected that all these conditions are uniquely interrelated irrespective of the magnitude of the cyclic load. As a simple example, the size of the crack tip plastic zone is not uniquely related to the size of the crack. This plastic zone at the same crack length will be larger for a high S_{max} than for a low S_{max} . Already in the crack nucleation period, microplasticity does not occur in the same way for any stress amplitude. The description of fatigue damage is complex. It certainly cannot be characterized by a single damage parameter. It implies that fatigue damage increments induced by load cycles will depend on the fatigue damaged condition of the material as caused by previous cycles. These effects are called *interaction effects*. The damage increment in a load cycle is depending on the size of the load cycle, but at the same time, it is affected by the damage caused by preceding cycles. The interaction effects are responsible for the *sequence effects* discussed before. As a result of the interaction effects it is difficult to arrive at a rational fatigue life prediction method for VA loading. Prediction models cannot be developed without simplifications. But several drastic simplifications have been proposed in the literature.

The most well-known simplified model of Miner was discussed before. Fatigue damage was supposed to linearly increase during CA cycles (see Figure 10.5a), also in blocks of cycles of VA loading, and without any interaction effects. In 1956 Shanley has proposed that fatigue damage should be defined as the size of a fatigue crack [5]. Crack initiation was supposed to start at the beginning of the fatigue life, and crack growth was supposed to be an exponential function, thus a non-linear function, see Figure 10.5b.

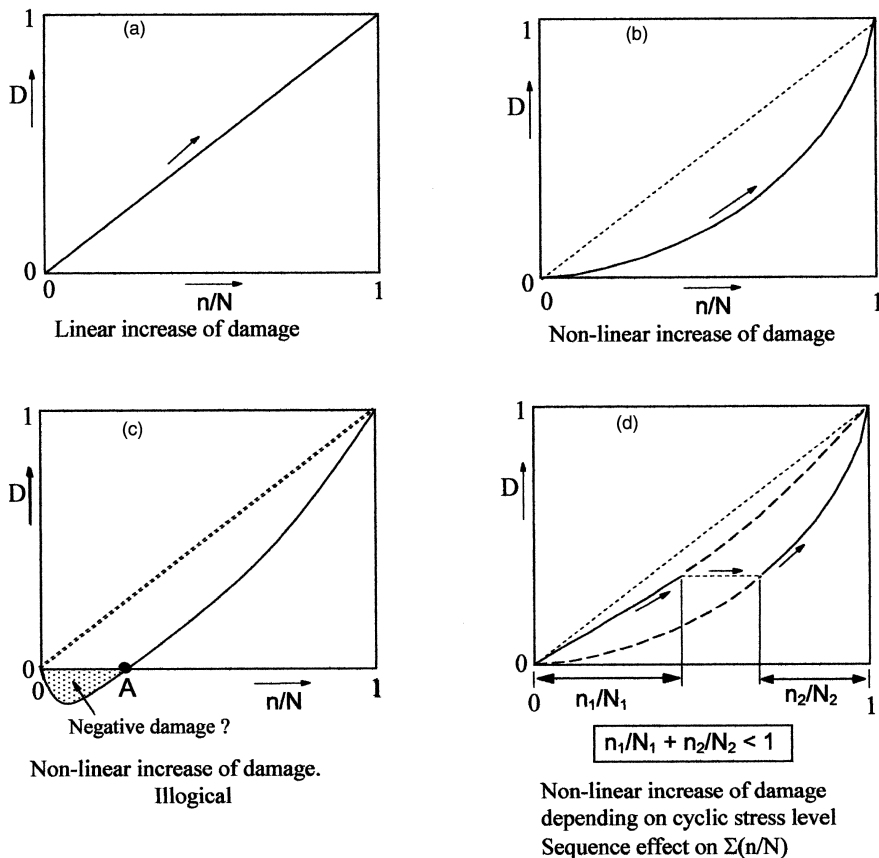


Fig. 10.5 Increasing fatigue damage characterized by a single damage parameter [6].

Shanley also thought that this function applied to all cyclic stress levels. It implies again that increasing damage during VA loading is moving along the damage curve from $D = 0$ to $D = 1$. Because Shanley also ignored interaction effects, his damage definition again leads to the Miner rule. Actually this applies to any non-linear damage function $D(n/N)$ if interaction effects are ignored.

A note about the $D(n/N)$ function should be made here. The function must be a monotonously increasing function. After it was recognized that a high load on a notched specimen can increase the fatigue life the term “negative damage” was used. The $D(n/N)$ function should show a curve with negative damage, see Figure 10.5c. After an initially decreasing part in the curve, it returns to $D = 0$ in point A. It should imply that the specimen is again undamaged condition, which appears to be illogical [6].

A different situation occurs if a damage function $D(n/N)$ is depending on the cyclic stress level, see Figure 10.5d. Now a sequence effects can occur. This is illustrated in this figure for a simple VA tests with two blocks of CA cycles, a stress history previously shown in Figure 10.1. During the first block, the damage parameter D increases along the upper curve. Changing over to the second block of small cycles implies a transition to the other damage curve to be followed until failure at $D = 1$. The sum of the two n/N contributions is obviously smaller than 1. The reversed sequence of the two blocks starting with the small cycles would lead to $\sum n/N > 1$.

Models with a non-linearly increasing single damage parameter have not led to an improved Miner rule giving reliable predictions with some general validity. Actually, the single damage parameter is in conflict with the present understanding of fatigue damage as it can accumulate under VA loading. The three shortcomings of the Miner rule discussed in the three previous sections are not removed by assuming a non-linear damage function.

In the previous sections it was shown that sequence effects could be explained as a consequence of plasticity effects, residual stress and the size of fatigue cracks. They all can contribute to the invalidity of the Miner rule. The problem of predicting fatigue lives under VA loading is a question of how fatigue damage is accumulating. The fundamental question is how fatigue damage should be defined. It is obvious that the microcracks or macrocracks must be part of the definition. At the same time, the discussion on the sequence effects indicate that plastic deformation and residual stresses should also be involved in the definition of fatigue damage. Although the significance of these aspects is evident in a qualitative way, it is also clear that a physical definition of fatigue damage in quantitative terms must be problematic. However for sure, fatigue damage cannot be defined by a single damage parameter.

In view of the complexity of defining the concept of fatigue damage, it is not strange that simplifications have been proposed for engineering purposes. And that was what Palmgren did in 1923. Nevertheless, it is useful to realize that the Miner rule is a rather drastic simplification which sometimes can lead to substantially wrong predictions as will be discussed later. Some alternative prediction models are described in Section 10.4, but first trends observed in VA tests are discussed.

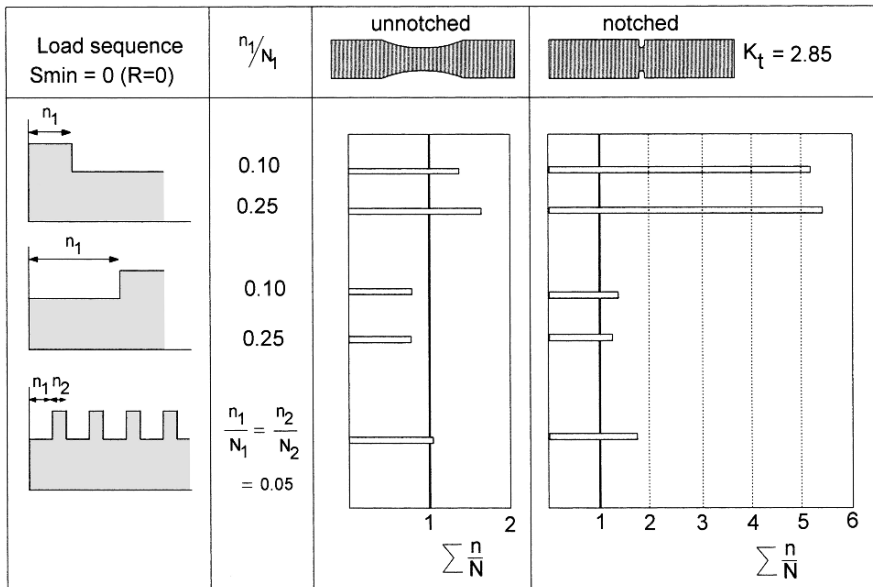


Fig. 10.6 Sequence effects in VA tests on unnotched and notched specimens of an Al-alloy (2024-T3) [7]. $S_{min} = 0$.

10.3 Results of fatigue tests under VA loading

Large numbers of VA tests were carried out in the 1950s and 1960s to verify the Miner rule. Relatively simple load histories were used, partly because simple sequences could very well indicate possible deviations from $\sum n/N = 1$. Another argument was that the fatigue testing machines present in the laboratories in those days could apply only simple load sequences to specimens. More complex sequences as shown in Figures 9.23 and 9.25 were not yet possible. These load histories were applied later, starting around 1970, when closed-loop electro-hydraulic testing systems were introduced (see Chapter 13). In spite of the limitations of the older machines, much has been learned about fatigue damage accumulation under VA loading with simple load sequences.

Some illustrative test results of simple VA fatigue tests ($S_{min} = 0$) are presented in Figure 10.6. Results of the notched specimens are considered first. Large values of $\sum n/N (>5)$ are found for the HiLo sequence. This should be associated with compressive residual stresses at the notch root introduced by the first block at a high S_{max} ($= 10^3$ MPa and $N = 185$ kc). In the LoHi sequence tests with the low S_{max} block applied first ($S_{max} =$

64 MPa and $N = 1200$ kc), the damage contribution in this block is negligible. Fatigue occurred predominantly in the second block with the high amplitude, which leads to $\sum n/N$ -values slightly above 1. An intermediate $\sum n/N$ -value ($\sum n/N = 1.8$) was found for the third load sequence with alternating low and high S_{\max} blocks.

Results of the unnotched specimens in the same figure show similar trends, but the deviations from $\sum n/N = 1$ are significantly smaller than for the notched specimens. Macroplasticity does not occur in the unnotched specimens, which excludes this mechanism for large sequence effects. In general, large $\sum n/N$ -values have not been reported for unnotched specimens, but values significantly smaller than one are mentioned in the literature. In the older days, low $\sum n/N$ -values were found for unnotched rotating beam specimens of steel.

Results of another test series on riveted lap joints are shown in Figure 10.7. The stress history consists of periods with blocks of four or five different amplitudes, applied in an increasing amplitude sequence, and superimposed on a positive mean stress (88 MPa). The number of cycles in one period is 433000 cycles. The result for series A is $\sum n/N = 1.3$. The stress history of series C was obtained from the history of series A by adding a small block (175 cycles) with a higher stress amplitude, which increased S_{\max} in the test. In view of the positive mean stress, it implies that more favorable compressive residual stresses could be developed in test series C. As a result, the fatigue life was more than doubled; $\sum n/N$ increased from 1.3 to 2.9. If the Miner rule would be correct, then the life in series C should be slightly shorter than in series A because of some damage added by the more severe load cycles.

The blocks in each period of series A and B are the same, but a single severe peak load cycle is added at the end of each period in series B. This cycle starts with a large negative amplitude, followed by the same positive amplitude. The latter peak load introduced significant compressive residual stresses, and as a result the life is increased considerably (factor six times). However, the Miner rule predicts a very small life reduction caused by the small number of peak load cycles.

A large peak load cycle was also added in series D to the fatigue loading of series C. However, this cycle now starts with the positive amplitude followed by the negative one, which leads to a significant reduction of the fatigue life. Apparently, the negative peak load has introduced tensile residual stresses, and eliminated the compressive residual stresses of the preceding positive peak load. The residual stresses in the test series

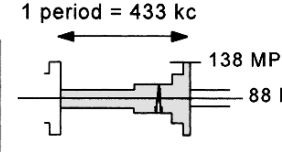
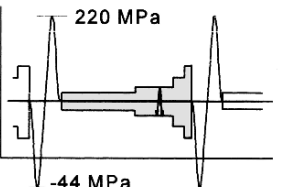
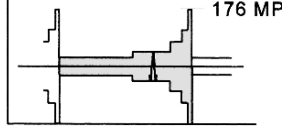
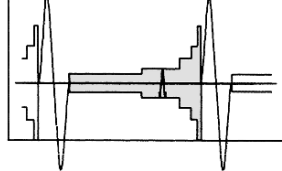
Series	Stress history	Life (periods)	$\sum \frac{n}{N}$
A	 <p>1 period = 433 kc</p> <p>138 MPa</p> <p>88 MPa</p> <p>4 amplitudes per period</p>	14	1.3
B	 <p>220 MPa</p> <p>-44 MPa</p> <p>As above, but one large cycle added, <u>neg./pos.</u></p>	85	7.8
C	 <p>176 MPa</p> <p>5 amplitudes per period</p>	31	2.9
D	 <p>As above, but one large cycle added, <u>pos./neg.</u></p>	11	1.1

Fig. 10.7 Effect of stress history on fatigue life and $\sum n/N = 1$. Results of VA fatigue tests on riveted lap joints (material 2024-T3 sheet) [8]. $S_m = 88$ MPa.

of Figure 10.7 reveal a similar effect as discussed earlier in relation to Figure 10.4. The explanation of the highly different results in Figure 10.7 in terms of residual stress effects is probably not fully complete because a riveted lap joint is a complicated notched specimen. But the highly different fatigue lives clearly demonstrate large load history effects which are fully outside predictions by the Miner rule.

Gassner has introduced the so-called block-program fatigue test already in 1939 [9]. He varied the stress amplitude periodically around a constant mean stress, see Figure 10.8. Gassner recognized that fatigue tests should also be carried out with a variation of the amplitude in agreement with load spectra observed in service. The loading program in Figure 10.8 covers 500000 cycles in one program period distributed over eight amplitudes in agreement

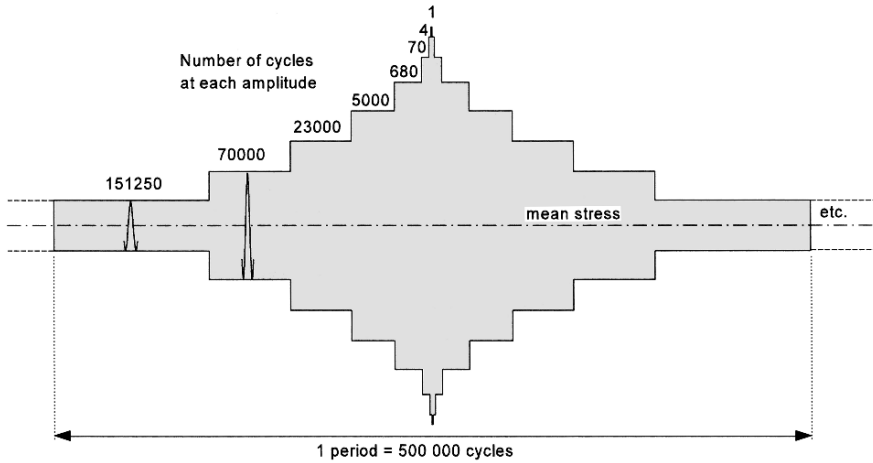


Fig. 10.8 Block program fatigue tests, introduced by Gassner [9], consisting of a low-high-low sequence of blocks of CA cycles.

with a load spectrum of aircraft wings. This low-high-low sequence (LoHiLo) of blocks of CA cycles is repeated until failure. The prime purpose was to adopt a load sequence that should be more representative for practical fatigue problems. However, the program fatigue test has also been used to check the Miner rule. Various test series are reported in the literature for block program tests with the same blocks in a period, but different sequences of the blocks. As an example, Figure 10.9 shows results of a NASA investigation on edge notched specimens ($K_t = 4.0$) [10]. It clearly illustrates that $\sum n/N$ depends on the sequences in which the blocks are applied. Secondly, it also shows that an increased mean stress leads to higher $\sum n/N$ -values. In a symmetric spectrum of amplitudes around a tensile mean stress, the maximum stress in a period is a larger tensile stress than (the absolute value of) the minimum compression stress in the same period. This promotes the development of favorable residual compression stresses due to notch root plasticity, which then leads to higher $\sum n/N$ -values as illustrated by the effect of the mean stress (S_m) in Figure 10.9.

Around 1970 closed-loop electro-hydraulic fatigue machines were introduced in fatigue testing laboratories. It then was possible to apply load time histories to specimens and structures, which could be defined as a computer command signal. Any sequence of load peaks, maxima and minima could be applied in a fatigue test, such as pure random loading histories (see Figure 9.18), or combinations of a deterministic load

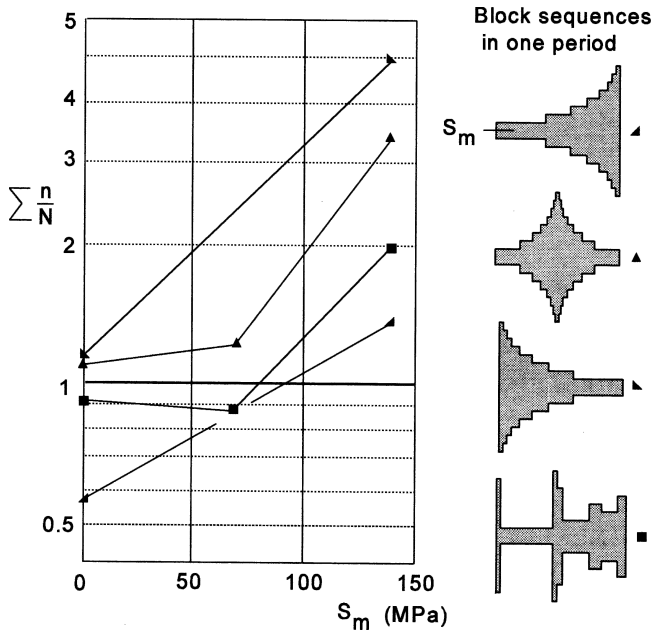


Fig. 10.9 Results of block-program fatigue tests of NASA [10]. Notched specimens, $K_t = 4$, material 7075-T6. Different block sequences and effect of mean stress.

(air-ground-air transitions) with a superimposed random loading as shown in Figure 9.25. The computer commands the fatigue load in the fatigue machine.

The sequence of load amplitudes during a random load history is significantly different from the sequence in block-program fatigue tests with the stress amplitude and the mean load remain constant during substantial numbers of cycles in each block. In a random load tests, and also in service, the amplitude varies from cycle to cycle. It must be expected that sequence effects and load cycle interaction effects are different in these two types of load histories. Experimental comparisons indeed showed different fatigue lives obtained under block-program loading and random load histories with the same load spectrum [11]. In general, fatigue lives in block program tests were longer than under equivalent random gust loading. Differences varied from relatively negligible to a 6 times longer life under block-program loading. It implies that a block-program fatigue test may give an unconservative indication of the fatigue life under more realistic random load sequences. The discrepancies between the results of the two types of fatigue tests have considerably affected the appreciation of realistic service-load-simulation fatigue tests. At the same time, the

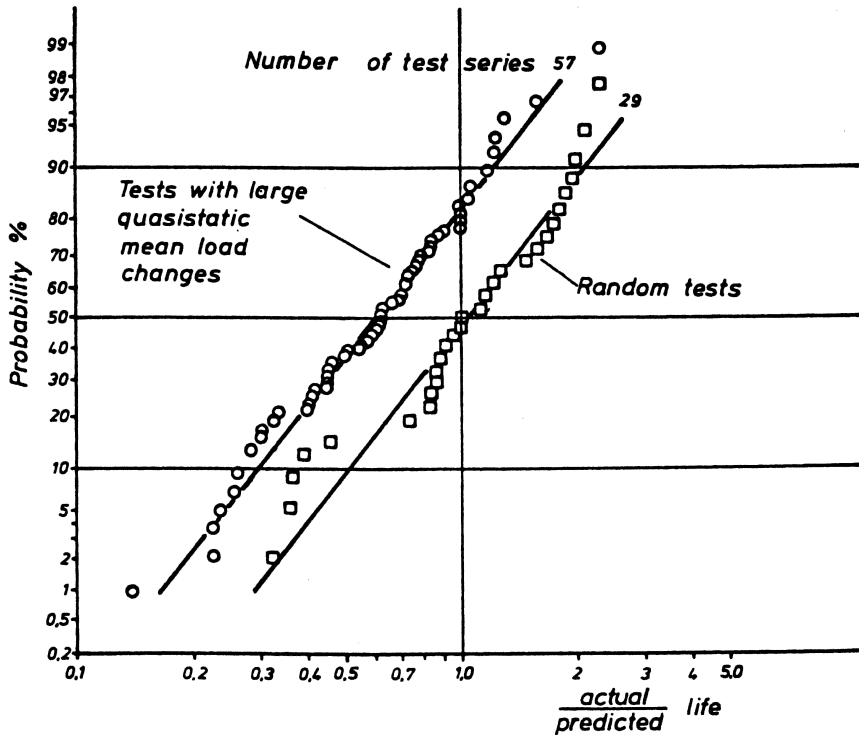


Fig. 10.10 Comparison between test results and predictions on fatigue lives in VA fatigue tests. Data collected by Schütz [12].

significance of the fatigue life indications obtained with the Miner rule were also questionable.

Schütz [12] made an analysis of $\sum n/N$ -values obtained in various tests series reported in the literature. He considered two groups of load sequences, viz. sequences with large variations of the mean stress in addition to amplitude changes (57 test series, mainly non-randomized), and sequences with a constant mean stress and a random variation of the load amplitude (29 test series), see Figure 10.10. The (logarithmic) horizontal scale gives the experimental life divided by the Miner-predicted life. This ratio is the experimental $\sum n/N$ -value. Along the vertical axis Schütz used the probability scale of the normal distribution function. It illustrates the scatter of $\sum n/N$ -values obtained in different test programs.¹⁴ In the large number of 57 test series, the average value is $\sum n/N = 0.6$, but $\sum n/N$ varies from

¹⁴ It should be understood that this scatter is not illustrating scatter between similar tests, but rather scatter between average results obtained in tests with different VA load sequences.

0.15 to 2.0. In the random load tests, the average value is $\sum n/N = 1.05$, while individual values range from 0.3 to 3.0.

The question should be raised why such large deviations of $\sum n/N = 1$ can occur. As pointed out earlier, shortcomings of the Miner rule can be qualitatively understood. Low values of $\sum n/N$ are possible if many small cycles are present in the load history, and if a zero mean stress is applicable. High $\sum n/N$ -values can be obtained if the load history has a positive mean stress, which promotes the possible occurrence of favorable residual stresses at notches (i.e. compressive residual stresses). The favorable residual stress effect is absent for unnotched specimens. Because of this qualitative understanding, it should not be a surprise that significant deviations from the Miner rule are observed.

10.4 Alternative fatigue life prediction methods for VA loading

10.4.1 Damage calculations and extrapolation of S-N curves below the fatigue limit

As pointed out earlier, an essential shortcoming of the Miner rule is due to ignoring damage contributions of load cycles with amplitudes below the fatigue limit. It then appears to be reasonable to extrapolate S-N curves to lower stress amplitudes with $S_a < S_f$ in order to assign some damage increments to cycles with amplitudes below the fatigue limit. Such an extrapolation is made in Figure 10.11, see line B. It implies that the Basquin relation, $S_a^k \cdot N = \text{constant}$, is assumed to be applicable for all fatigue cycles with stress amplitudes below the fatigue limit. The effect of this extrapolation will be illustrated by life calculations with the Miner rule. The calculations are made for two load spectra, H_1 and H_2 shown in Figure 10.11. The calculation for spectrum H_1 is presented in Table 10.1. The first column of the table gives S_a -values for which the number of exceedings (spectrum for 5000 hrs) is read in Figure 10.11. The incremental number $n = \Delta H$ is the number of cycles for the corresponding S_a intervals. The fatigue life N for the median stress level of this interval is read from the S-N curves in the same figure. Damage increments n/N can then be calculated, which are presented in the last two columns of the table for S-N curves A and B respectively. The sum of these increments is $\sum n/N$ for 5000 hrs. The fatigue life until failure according to the Miner rule is then obtained as soon as $\sum n/N = 1$, which leads to

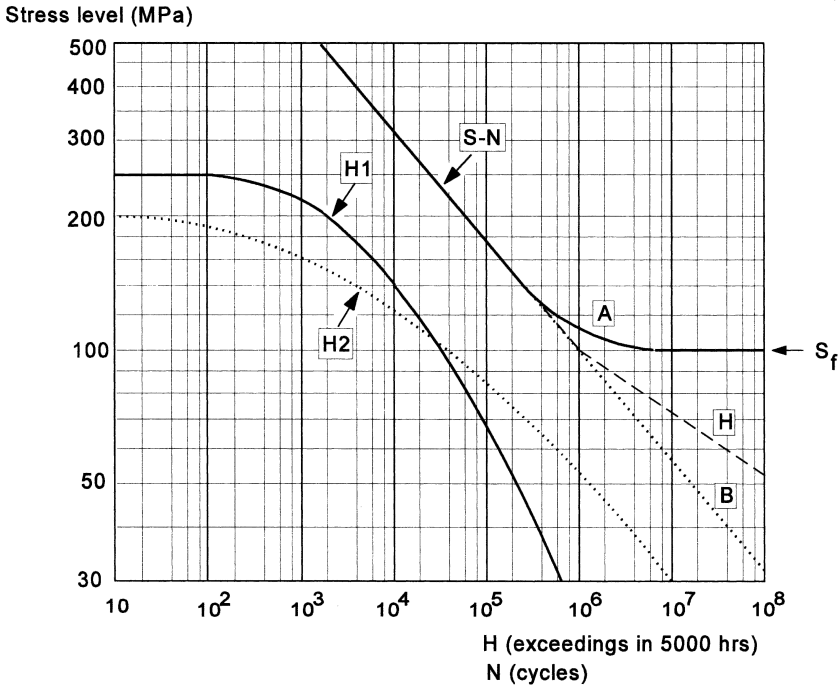


Fig. 10.11 Two load spectra and an S-N curve in a Miner calculation.

$$\text{Life} = \frac{1}{\sum \frac{n}{N}} * 5000 \text{ hrs} \tag{10.3}$$

The results for the two S-N curves are shown at the bottom of Table 10.1. Smaller increments of S_a can be used, which makes the calculation more precise, but not necessarily more accurate because it is based on the validity of $\sum n/N = 1$ at failure. If the load spectrum and the S-N curve can be given in analytical format by $H(S_a)$ and $N(S_a)$, then $\sum n/N$ can be numerically calculated by integration of $dD = dH(S_a)/N(S_a)$ and again:

$$\text{Life} = \left(\frac{1}{D} \right) * 5000 \text{ hrs}$$

Calculated fatigue lives based on the S-N curves A and B for both spectra H_1 and H_2 are summarized in Table 10.2. The results confirm that the calculated fatigue life is significantly shorter if the Miner prediction is based on the extrapolated S-N curve B which then includes fatigue damage of cycles with $S_a < S_f$. The effect is much larger for spectrum H_2 with relatively

Table 10.1 Damage calculation for spectrum *H* in Figure 10.11.

Spectrum <i>H</i>			S-N data			Damage calculation	
<i>S_v</i> (MPa)	<i>H</i> (cycles)	<i>n = ΔH</i>	Average <i>S_v</i> of interval	Corresponding <i>N</i> (cycles)		<i>n/N</i>	<i>n/N</i>
				Curve A	Curve B	Curve A	Curve B
250	100	450	240	30000	30000	0.015	0.015
230	550	700	220	43000	43000	0.0162	0.0162
210	1250	1150	200	62500	62500	0.0184	0.0184
190	2400	1900	180	95000	95000	0.02	0.02
170	4300	3200	160	150000	150000	0.0213	0.0213
150	7500	6000	140	260000	260000	0.0231	0.0231
130	13500	11500	120	600000	600000	0.0192	0.024
110	25000	21000	100	107	106	0.0021	0.021
90	46000	49000	80	-	2.4×10 ⁶	-	0.0204
70	95000	125000	60	-	7.5×10 ⁶	-	0.0167
50	220000	480000	40	-	40×10 ⁶	-	0.012
30	700000	4300000	20	-	625×10 ⁶	-	0.0069
10	5000000						
<i>H</i> = number of exceedings in 5000 hrs						<i>D_A</i> = Σ <i>n/N</i> = 0.1353	<i>D_B</i> = Σ <i>n/N</i> = 0.2150
			Calculated fatigue life: S-N curve A: Life = (1/ <i>D_A</i>) × 5000 = 37000 hrs S-N curve B: Life = (1/ <i>D_B</i>) × 5000 = 23000 hrs				

Table 10.2 Miner predictions.

S-N curve used	Fatigue life (hrs)		Life ratio (<i>H</i> ₁ / <i>H</i> ₂)
	Spectrum <i>H</i> ₁	Spectrum <i>H</i> ₂	
A	37000	66000	0.56
B	23000	7000	3.3
	B/A = 0.62	B/A = 0.11	

many cycles below the fatigue limit. A comparison between the severities of spectra *H*₁ and *H*₂ is made in the last column of Table 10.2. It indicates that the predicted fatigue life for spectrum *H*₁ is almost 50% shorter than for spectrum *H*₂ if S-N curve *A* is used, whereas it is 3.3 times longer if S-N curve *B* is adopted. In view of the results of Table 10.2, it must be concluded that the Miner rule is suspect to indicate differences between the severity of different load spectra.

The damage contributions calculated in Table 10.1 are plotted in Figure 10.12. It illustrates the distribution of the damage increments of the various load intervals, which has a maximum at a certain stress level. This

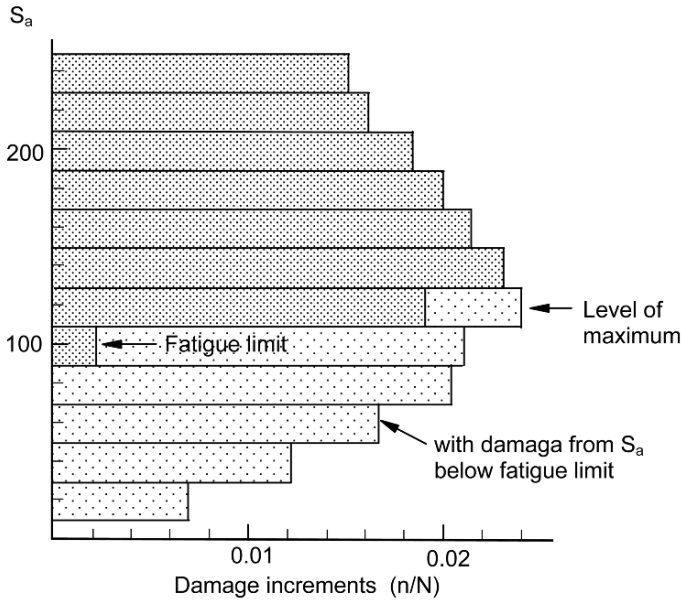


Fig. 10.12 Distribution of damage increments of a Miner calculation.

stress level has been labeled in the literature as the most damaging stress level of a load spectrum, but it should be recalled that this statement is entirely based on the Miner rule, and thus has a questionable meaning.

Another suggestion for extending the S-N curves below the fatigue limit was proposed by Haibach [13], which is line *H* in Figure 10.11. Haibach postulated that cycles with amplitudes above the fatigue limit will reduce the fatigue limit of the undamaged material. As a result, cycles with an amplitude $S_a < S_f$ are damaging. The damage of these cycles was accounted for by applying the Miner rule to a modification of the S-N relation by the extension with line *H* in Figure 10.11. According to Haibach, the slope of line *H* is related to the slope of the Basquin relation of the original S-N curve; $S_a^k \cdot N = \text{constant}$. In this equation, k should be replaced by $2k-1$. Of course, a prediction with this modified S-N curve is more conservative than the original Miner rule prediction, but less conservative than for the extended S-N curve with line *B*. Again, it must be recalled that the prediction with $\sum n/N$ remains a Miner rule prediction, which does not account for any interaction effect. Predictions must be considered with caution. The extrapolated S-N curves imply that an extra safety margin is introduced which intuitively seems to make sense, but it remains unknown how large

this margin is, and also whether the prediction will be conservative, i.e. $\sum n/N \geq 1$.

10.4.2 The relative Miner rule

Schütz [12] considered the unconservative predictions of the Miner rule, and he introduced the idea that systematic unconservative predictions could be accounted for by replacing $\sum n/N = 1$ by a “relative Miner rule”, $\sum n/N = q$, with $q < 1$. The value of q had to be selected by experience of VA tests with similar load-time histories relevant to the problem under consideration. The relative Miner rule can also be interpreted as using the Miner rule with a safety factor to account for possible unconservative life predictions. Although such a safety approach appears reasonable, Schütz also pointed out that realistic predictions require test results obtained under realistic load sequences to be applied to the structure or component itself.

10.4.3 Strain history prediction model

The previously discussed models try to predict the fatigue life under VA loading from fatigue lives obtained under CA loading, i.e. S-N curves. After it was realized that notch root plasticity could occur and would introduce a local residual stress distribution, it was tried to account for the real strain history at the root of the notch. It has led to fatigue predictions for VA loading based on the predicted strain history at the notch root [14, 15]. Such predictions came in focus when the Neuber postulate was developed for the prediction of residual strain and stress at the root of a notch. This postulate was discussed in Chapter 4 (Section 4.4). Furthermore, low-cycle fatigue experiments under constant-strain amplitudes have indicated an approximately linear relation between $\log \Delta \varepsilon$ and $\log N$ (the Coffin–Manson relation), discussed in Chapter 6 (Section 6.4). The procedures to be used for calculation of the strain history at the notch under VA loading, and for the subsequent life prediction are schematically shown in Figure 10.13. A detailed discussion of these procedures has been given by Dowling [15]. The main steps are mentioned here in order to see advantages and weaknesses of the approach.

In the first step (Figure 10.13a) the strain history $\varepsilon(t)$ is derived from the load history $P(t)$ by employing the Neuber postulate and the cyclic stress

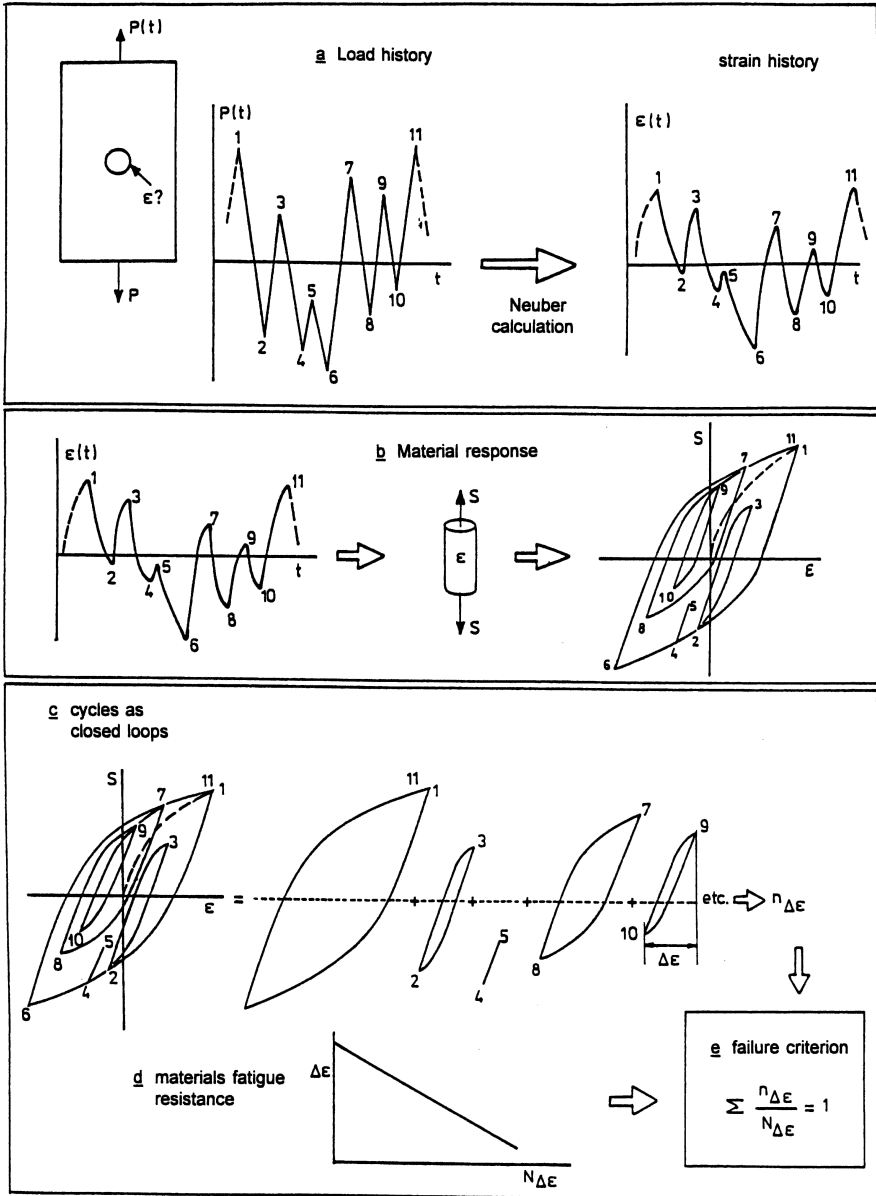


Fig. 10.13 Principles of the notch-root strain-based prediction model [14].

strain curve. In the second step, the σ - ε response of the material (at the root of the notch) is derived from $\varepsilon(t)$ (Figure 10.13b). It presumes a certain plastic hysteresis behavior based on the material memory for previous plastic deformation. In the third step (Figure 10.13c) the cyclic hysteresis history is decomposed into closed hysteresis loops. Each loop represents a full strain cycle. In the last step (Figures 10.13d and e) the $\Delta\varepsilon$ - $N_{\Delta\varepsilon}$ curve is used as the material property characterizing the material resistance against low-cycle fatigue. The Miner rule is then adopted as the failure criterion.

The material properties required for the strain-history model are the cyclic stress strain curve and the Coffin–Manson relation. Both types of data are considered to be unique for a material. This is an advantage over the stress based S-N fatigue data, which depend on mean stress and surface quality. The surface quality is much less important for low-cycle fatigue, because the plastic strains are larger and thus mainly depending on the material bulk behavior. Low-cycle fatigue is no longer a surface phenomenon as it is for high-cycle fatigue. At the same time, limitations of the strain-history model are easily recognized. The failure criterion is again the Miner rule, for which physical arguments can hardly be mentioned. Secondly, crack initiation and crack growth are fully ignored. Moreover, the model is restricted to notched elements, for which a theoretical stress concentration factor has a realistic meaning. As a consequence, application to joints is generally impossible. It was emphasized by Dowling [15] that the merits of the model should be looked for in low-cycle VA problems. Actually, verification experiments are still rather limited.

A noteworthy comment should be made on the decomposition in Figure 10.13c. The individual cycles obtained are the same cycles as obtained with the rain-flow count method. It implies that this counting method finds some justification in the material memory for previous plastic deformation.

10.4.4 Predictions based on service-simulation fatigue tests

The application of the Miner rule to fatigue life predictions implies that results of CA tests are extrapolated to conditions of VA load-time histories. In view of the limited validity of the Miner rule, an obvious approach is to look for predictions based on results of “relevant” VA tests, i.e. results of service-simulation fatigue tests discussed in the previous chapter (Section 9.5). Such tests should imply a much smaller extrapolation. Due

attention must then be paid to the notch effect, size effect, and effect of surface quality, aspects discussed in Chapter 8 (fatigue properties of notched elements). Specimens to be tested should be as much similar as possible to the real component, or the fatigue critical location of a structure. The most relevant service-simulation fatigue test is a test on the structure or a component itself. This is sometimes done, noteworthy in the automotive industry and the aircraft industry. However, if such a test meets with practical problems, a service-simulation fatigue test on a representative specimen can give useful indications on the fatigue performance of a structure.

An additional and important question is: which load-history should be used in service-simulation fatigue tests for prediction problems? The load spectrum, and also the load sequence in the test should be representative for conditions expected in service. A block-program fatigue test discussed before cannot be considered to be a good choice. Randomness of loads in service should be simulated in the test, which is experimentally very well possible with modern fatigue machines. Service-simulation fatigue tests for aircraft structures, referred to as flight-simulation fatigue tests, have been extensively used for various purposes. An example of the load history applied in such a test was shown in the previous chapter (Figure 9.25). The stress-history was characterized by one specific stress level, for which the mean stress in flight (S_{mf}) was chosen. If the design stress level of the structure is increased (or decreased), all cyclic stress levels are changed proportionally, and thus S_{mf} remains a characteristic stress level for the intensity of the stress history. Fatigue life results of flight-simulation fatigue tests, carried out at different values of the characteristic stress level S_{mf} , can then be plotted as a function of S_{mf} . Such fatigue life curves are presented in Figure 10.14. Similar plots can be made for other types of stress histories. Figure 10.15 shows a fatigue life curve for pure random loading with the root-mean-square of the stress (S_{rms}) as the characteristic stress level of the load history.

It is noteworthy that experimental results of service-simulation fatigue tests suggest a linear relationship between the stress level and the fatigue life plotted on a double log scale. It implies that the Basquin relation should again describe the effect of the cyclic stress intensity:

$$(S_{\text{characteristic}})^k \cdot \text{life} = \text{constant} \quad (10.4)$$

Moreover, it appears that the slope factor k is of the same order of magnitude as the slope factor for S-N curves. Intuitively, the latter observation about the effect of the stress level seems to be plausible, but a firm proof would require a valid model for fatigue damage accumulation, which in fact is not available.

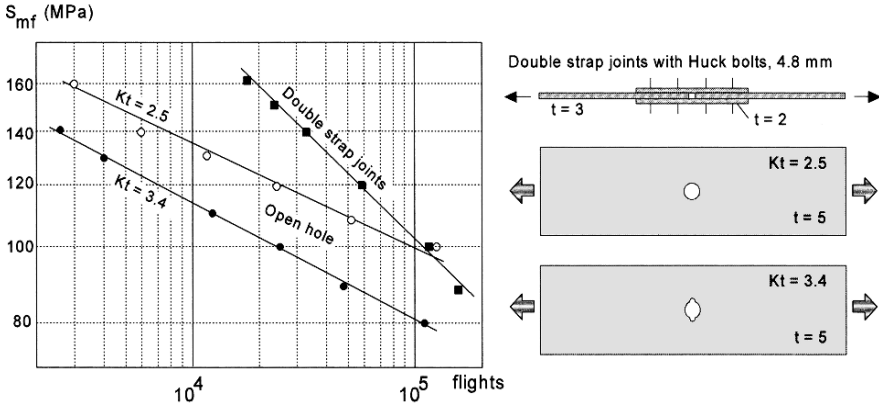


Fig. 10.14 Results of flight-simulation fatigue tests on notched specimens of an Al-alloy (2024-T3) [16]. The data points follow the Basquin relation (Eq. 10.4). Thickness t in mm.

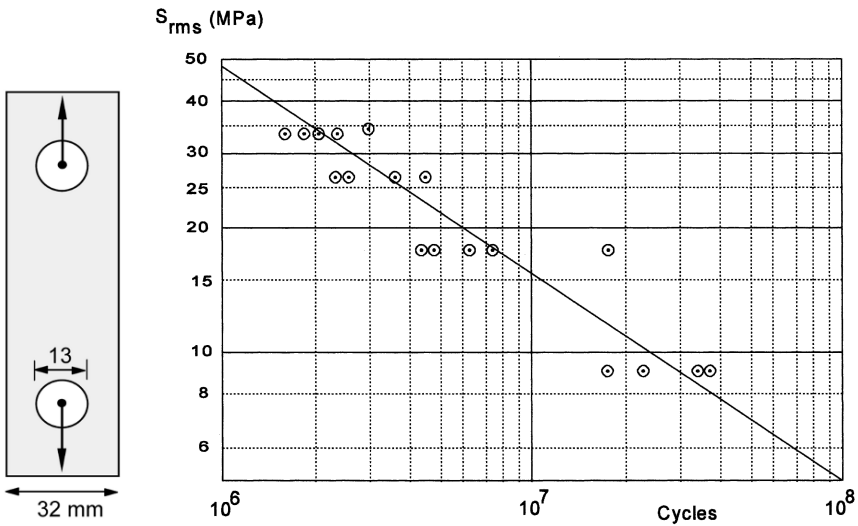
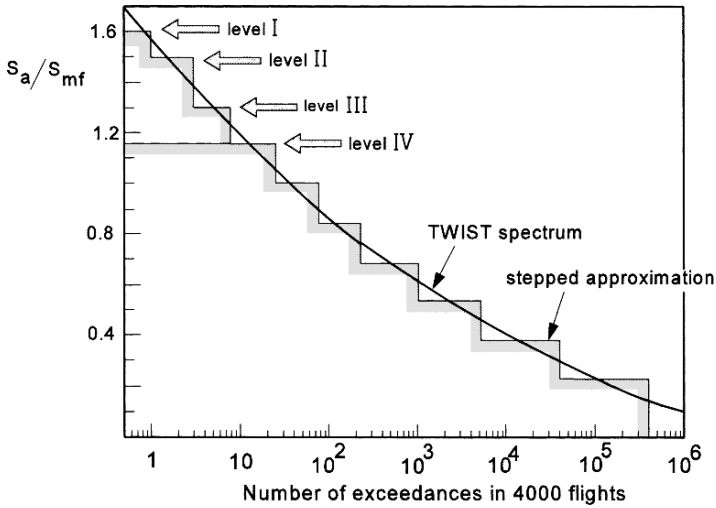
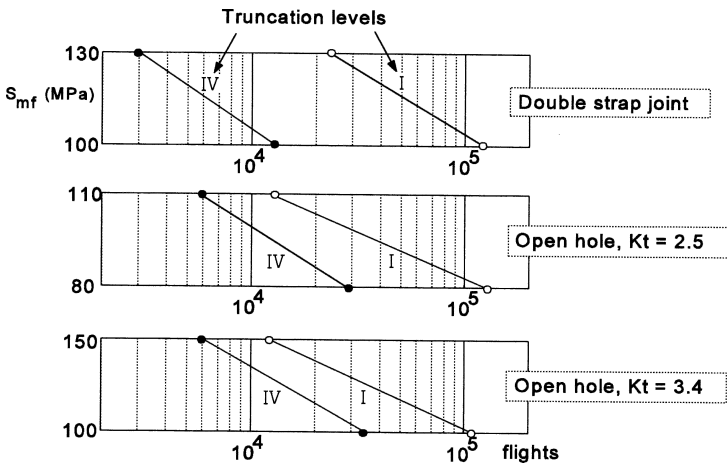


Fig. 10.15 Results of narrow band random load tests on lug specimens. Fatigue life as a function of the root-mean-square value of the stress amplitude; mean stress 108 MPa [17].

The analysis of a large number of flight-simulation tests on Al-alloys [18] indicated slope values around $k \approx 5$. The effect of the design stress level under service-simulating fatigue loading can be estimated with this slope factor. As an example, if $k = 5.0$, an increase of the design stress level with 20% would reduce the life with a factor equal to $1.2^5 = 2.5$. If k for fatigue life curves under VA loading is not available, a k -value can be adopted from S-N curves for a similar notch geometry and material.



(a) The stress amplitude distribution of the TWIST load spectrum.
 S_{mf} = mean stress in flight, see Figure 9.25



(b) Tests results with the effect of the truncation level

Fig. 10.16 The effect of truncating high-amplitude cycles of a steep spectrum (TWIST) in flight-simulation fatigue tests (similar specimens as in Figure 10.14) [15]. Large truncation effect.

In the previous chapter (Section 9.5), the significance of truncating high-amplitude cycles of a load spectrum was mentioned. As suggested, the influence could be large for a steep spectrum. This is illustrated by the results of Figure 10.16. The tests were carried out with the standardized TWIST spectrum, a spectrum for transport aircraft wing structures with

mainly gust loads in flight. The spectrum given in Figure 10.16a is a steep spectrum. In the experiments it is approximated by the stepped function given in the figure. Truncation levels are numbered by Roman figures. Truncation at level I implies that the maximum level occurs once in 4000 flights. Truncation at the much lower level IV implies that the amplitude of cycles with a larger amplitude than level IV is reduced to level IV. As a consequence, the maximum amplitude becomes 72% of level I which now occurs 18 times in 4000 hours. The experimental results in Figure 10.16b show that the truncation has led to a significant reduction of the fatigue life until failure. This large truncation effect is not predicted by the Miner rule. On the contrary, the Miner rule predicts a slight increase of the fatigue life by the truncation instead of the significant reduction. Truncation of a steep spectrum is advised in order to obtain conservative test results. Under service conditions, the rarely occurring high amplitudes will not be encountered by all structures in service because of statistical variation of the load spectrum. The life-increasing effect of the rarely occurring high loads will thus not apply to all structures. The choice of a truncation level for a steep load spectrum remains a precarious question which should be answered by considering the variability of the load spectrum in service. Furthermore, it can be instructive to carry out service-simulation tests on representative specimens using some different truncation levels in order to explore the sensitivity for this variable.

Fortunately, the spectrum truncation problem is less important for flat load spectra with relatively many high-amplitude cycles. All structures will meet some high-amplitude cycles. Moreover, the relatively small number of low-amplitude cycles of a flat spectrum are less important for the accumulated fatigue damage. Experimental results in Figure 10.17 for a flat maneuver spectrum still show a systematic truncation effect, i.e. shorter fatigue lives for a truncated spectrum, but the effect is much smaller than in Figure 10.16 for a steep spectrum.

In spite of the truncation problem, results of service-simulation fatigue tests are much more significant than results obtained by Miner rule predictions based on S-N curves. The reliability of these predictions is not only depending on the doubtful validity of the Miner rule, but also on the estimated S-N curves. If tests for prediction problems are considered to be desirable, service-simulation tests are more instructive than constant-amplitude tests.

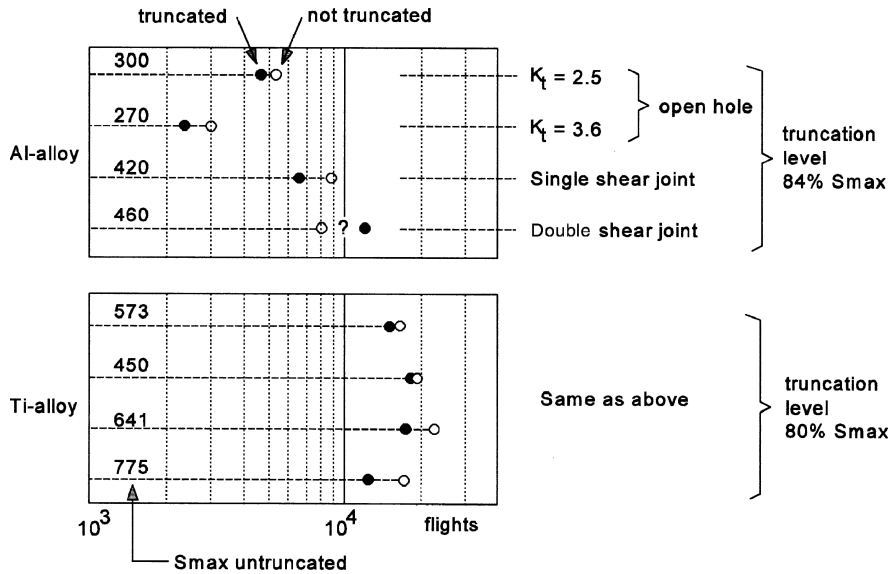


Fig. 10.17 Effect of truncating high-amplitude cycles of a flat maneuver load spectrum (FALSTAFF) in a flight-simulation fatigue test [19]. Specimens of an Al-alloy (2024-T3) and a Ti-alloy (Ti-6Al-4V). Small truncation effect.

10.5 Discussion of fatigue life predictions for VA loading

Results of VA fatigue tests clearly indicate that the Miner rule does not give accurate and reliable predictions on fatigue lives. The shortcomings can be understood. Two major objections are: (i) cycles with an amplitude below the fatigue limit do not contribute to fatigue damage, and (ii) the second one, notch root plasticity leads to interaction effects between cycles of different magnitudes which are not accounted for in the Miner rule. The first objection can be alleviated by extending S-N curves below the fatigue limit. The linear extrapolation curve B in Figure 10.11 is probably a conservative approach. But according to the present understanding of fatigue damage accumulation, it cannot be concluded that the problem is solved on rational grounds. The significance of the second shortcoming (notch root plasticity) can also be understood. Although it can be tried to account for this deficiency by sophisticated plasticity calculations, the Miner rule still ignores load cycle interactions. The only realistic approach for predicting fatigue lives of structural components is to rely on results of service-simulation fatigue tests. In view of this conclusion, the perspectives of the Miner rule ($\sum n/N = 1$) and service-simulation fatigue tests are reconsidered here

in relation to different applications to fatigue prediction problems of VA loading. The following topics are addressed:

1. Life estimates for a specific component and the Miner rule.
2. Considerations on the effect of the design stress level.
3. Comparison between different options for design improvements (materials, notch geometries, joints, surface treatments).
4. Comparison of different spectra (different utilizations of the same structure).

10.5.1 Life estimates for a specific component and the Miner rule

The Miner rule $\sum n/N = 1$ can only give a rough estimate of the fatigue life. It is a kind of averaging the severity of the various load cycles of the load spectrum. Extrapolation of S-N curves to low amplitudes must be advised anyway. Predictions may still be considered to be reasonable if the deviation of the real life from the predicted life is no more than a factor 2, i.e. that it should be between 50% and 200% of the prediction. However, if a designer is using the Miner rule, he should realize that the accuracy of the prediction is not only depending on the Miner rule, but also on the relevance of the S-N curves used for the prediction. The designer may well keep in mind that the Miner rule may be more safe if a positive mean stress applies to the load spectrum and less safe for a zero mean stress. The latter case applies to rotating bending of axles where notch plasticity is generally not allowed. Furthermore, the applicability of the Miner rule will be more uncertain for steep load spectra and probably less uncertain for a flat load spectrum. Actually a flat load spectrum is more close to CA loading, and interaction effects will be less significant.

Whether an estimated life obtained with the Miner rule is sufficient to exclude the need for realistic fatigue tests is a matter of engineering judgement. Uncertainties about the S-N curve, specific service conditions (e.g. corrosion) and possible consequences of premature fatigue failures have to be considered. Safety factors can be adopted, which in view of scatter will be advisable anyhow (see Chapters 13 and 20). Beyond any doubt, more reliable predictions are obtained from relevant service-simulation fatigue tests.

10.5.2 Considerations on the effect of the design stress level

As pointed out earlier, the effect of the design stress level can be taken into account by using the Basquin relation, Eq. (10.4). A Miner calculation will not give a reliable indication. According to literature data, k -values in the Basquin relation will be in the order of 4 to 6. A fatigue life reduction factor due to an increased design stress level is conservatively estimated by using a relatively high k -value, while a life improvement factor due to a reduced design stress level is conservatively estimated by a relatively low k -value.

If the fatigue life is largely covered by macrocrack growth, a low k -value should be adopted in the range of 3 to 4. This conclusion is associated with the exponent of the Paris crack growth relation as will be discussed in Chapter 11.

10.5.3 Comparison between different options for design improvements

The fatigue resistance of a component can be improved by selecting an other material, or changing the geometry of the notch (a larger root radius to reduce the local stress concentration), or adopting a different surface treatment (e.g. shot peening). If the Miner rule would be used for such comparisons, it implies that first comparative CA tests must be carried out. These data should then be used for Miner calculations. This approach cannot be considered to be a clever solution for VA problem settings. Comparative service-simulation fatigue tests are by far the best method and the most efficient one. Of course, if fatigue failures are inadmissible, then the fatigue limit is the important property, and CA tests should be used.

10.5.4 Comparison of different load spectra

The problem of comparing different spectra is important if structures can be used in different ways. This is easily understood for aircraft, motor vehicles, cranes and various other structures as well. It then is desirable to know whether different usages of the same structure will lead to significantly different fatigue lives in service. Unfortunately, the Miner rule is unreliable to answer these questions. Some illustrations were presented in the previous sections. For instance, the effect of load cycles with a high S_{\max} can have

a large favorable effect, whereas the Miner rule predicts a small reduction. Furthermore, the discussion in Section 10.4.1 on the comparison between two different load spectra H_1 and H_2 in Figure 10.11 indicated that the Miner rule did not give an unambiguous result. It must be emphasized that experimental evidence is indispensable for the comparison of the severity of different load spectra. It should be obtained in realistic service-simulation fatigue tests on representative specimens.

10.6 Major topics of the present chapter

The major topics of this chapter are fatigue damage accumulation under Variable-Amplitude (VA) loading, the Miner rule and life predictions for VA loading. The present chapter is dealing with fatigue life until failure including the initiation period. Crack growth of macrocracks under VA loading is considered in Chapter 11. The more significant aspects of the present chapter are listed below:

1. The most simple method for fatigue life predictions is to use the Miner rule, $\sum n/N = 1$. Unfortunately, this rule is not reliable, because of some elementary shortcomings. Two important deficiencies are: (i) Cycles with a stress amplitude below the fatigue limit are supposed to be non-damaging. In reality, these cycles can extend fatigue damage created by cycles with amplitudes above the fatigue limit. (ii) Notch root plasticity leads to residual stresses which can affect the fatigue damage contribution of subsequent cycles. This interaction effect is also ignored by the Miner rule.
2. The Miner rule and several other prediction models assume that fatigue damage can be fully characterized by a single damage parameter ($\sum n/N$ in the Miner rule), which is physically incorrect. Fatigue damage also includes local plasticity and residual stress.
3. Results of $\sum n/N$ -values at failure quoted in the literature vary from much smaller than 1 to significantly larger than 1. Small values are promoted by unnotched specimens and a zero mean stress. High values are prompted by notched specimens in combination with a positive mean stress, and also by steep load spectra (low numbers of severe load cycles). Residual stresses are important to explain high $\sum n/N$ -values.
4. The sequence of different load cycles in a VA load history can have a large effect on $\sum n/N$ at failure. This is more true for block-program fatigue load sequences than for sequences with random

- loads or mixtures of deterministic and random loads. Block-program tests should be discouraged for practical problems.
5. If fatigue life predictions are made with the Miner rule, it should be realized that the results are associated with uncertainties of the reliability of the rule, and also with the relevance of the S-N curves adopted. If the Miner rule is still adopted, it must be recommended to extrapolate S-N curves below the fatigue limit in order to assign fatigue damage contributions to small cycles below the fatigue limit. At best, the Miner rule gives a rough estimate of the fatigue life.
 6. Improvements of life prediction methods have been proposed in the literature, but it is still questionable whether they offer a good solution for practical design problems.
 7. The only reasonable alternative is to obtain test results of relevant service-simulation fatigue tests. Such tests should be relevant with respect to the material, notch configuration and material surface condition, as well as the load history expected in service.
 8. Service-simulation fatigue tests are also recommended for comparative investigations of materials, surface treatments, joints and components in general, and also for comparing the severity of different load spectra. The Miner rule is not reliable for these purposes.

References

1. Pålmgren, A., *The fatigue life of ball-bearings*, Z. VDI, Vol. 68 (1924), pp. 339–341 [in German].
2. Langer, B.F., *Fatigue failure from stress cycles of varying amplitude*. J. Appl. Mech., Vol. 4 (1937), pp. A160–A162.
3. Miner, M.A., *Cumulative damage in fatigue*. J. Appl. Mech., Vol. 12 (1945), pp. A159–A164.
4. Wällgren, G., *Review of some Swedish investigations on fatigue during the period June 1959 to April 1961*. Report FFA-TN-HE 879, Stockholm (1961).
5. Shanley, F.R., *A proposed mechanism of fatigue failure*. Colloquium on Fatigue, Stockholm, 1956. W. Weibull and F.K.G. Odquist (Eds.), Springer, Berlin (1956), pp. 251–259.
6. Schijve, J., *Some remarks on the cumulative damage concept*. Minutes 4th ICAF Conference, Zürich (1956), paper 2.
7. Schijve, J. and Jacobs, F.A., *Fatigue tests on notched and unnotched clad 24 S-T sheet specimens to verify the cumulative damage hypothesis*. Nat. Aerospace Laboratory, NLR, Amsterdam, Report M.1982 (1955).
8. Schijve, J., *The endurance under program-fatigue testing*. Full-Scale Fatigue Testing of Aircraft Structures. Proc. ICAF Symposium, Amsterdam 1959, Pergamon Press (1961), pp. 41–59.

9. Gassner, E., *Strength experiments under cyclic loading in aircraft structures*. Luftwissen, Vol. 6 (1939), pp. 61–64 [in German].
10. Naumann, E.C., Hardrath, H.R. and Guthrie, E.C., *Axial load fatigue tests of 2024-T3 and 7075-T6 aluminum alloy sheet specimens under constant- and variable-amplitude loads*. NASA Report TN D-212 (1959).
11. Jacoby, G.H., *Comparison of fatigue lives under conventional program loading and digital random loading*. Effects of Environmental and Complex Load History on Fatigue Life. ASTM TP 462 (1970), pp. 184–202.
12. Schütz, W., *The prediction of fatigue life in the crack initiation and propagation stages. A state of the art survey*. Engrg. Fracture Mech., Vol. 11 (1979), pp. 405–421.
13. Haibach, E., *Modified linear damage accumulation hypothesis accounting for a decreasing fatigue strength during increasing fatigue damage*. Laboratorium für Betriebsfestigkeit, LBF, Darmstadt, TM Nr. 50 (1970) [in German].
14. Dowling, N.E., Brose, W.R. and Wilson, W.K., *Notched member fatigue life predictions by the local strain approach*. Fatigue under Complex Loading: Analysis and Experiments, R.M. Wetzel (Ed.), Advances in Engineering, Vol. 7, SAE (1977), pp. 55–84.
15. Dowling, N.E., *Mechanical Behavior of Materials. Engineering Methods for Deformation, Fracture, and Fatigue*, 3rd edn. Prentice-Hall (2006).
16. Schütz, D. and Lowak, H., *The application of the standardized test program for the fatigue life estimation of transport aircraft wing components*. Proc. ICAF Symp., Lausanne, Paper 3.64 (1975).
17. Kirkby, W.T., *Constant-amplitude of variable-amplitude test as a basis for design studies. Fatigue design procedures*, ICAF Symp., 1965, Munich 1965, E. Gassner and W. Schütz (Eds.), Pergamon Press (1969), pp. 253–290.
18. Schijve, J., *The significance of flight simulation fatigue tests*. Durability and Damage Tolerance in Aircraft Design, ICAF Symp. Pisa, 1985, A. Salvetti and G. Cavallini (Eds.), EMAS, Warley (1985), pp. 71–170.
19. Lowak, H., Schütz, D., Hück, M. and Schütz, W., *Standardized flight-simulation programme for fighters: FALSTAFF*, LBF-Report 3045, IABG Report TF, 568 (1976) [in German].

Some general references (see also [12] and [18])

20. Rice, C.R. (Ed.), *SAE Fatigue Design Handbook*, 3rd edn. AE-22, Society of Automotive Engineers, Warrendale (1997).
21. Schijve, J., *The accumulation of fatigue damage in aircraft materials and structures*. AGARDograph No. 157 (1972).